25. T. D. Palmer, E. A. Maskakis, A. R. Willoite, F. Safcor F. H. Gage, *J. Neurosci.* **19**, 8487 (2000).
26. W. Li, C. A. Cogswell, J. J. LoTurco, *J. Neurosci.* **18**, 8853 (1998).
27. F. Doetsch, I. Caille, D. A. Lim, J. M. Garcia-Verdugo, A. Alvarez-Buylla, *Cell* **97**, 703 (1999).
28. I. L. Weissman, *Cell* **100**, 157 (2000).
29. H. Geiger, S. Sick, C. Bonifer, A. M. Müller, *Cell* **93**, 1055 (1998).
30. Details of the culture conditions and immunostaining methods are available as supplementary material to *Science* Online subscribers www.sciencemag.org/feature/data/1051654.shl.
31. We thank A. Mudge and members of the Raff laboratory for advice and comments on the manuscript. T.K. was supported by a Japan Society for the Promotion of Science Postdoctoral Fellowship for Research Abroad. M.R. is supported by a Programme Grant from the Medical Research Council, UK.

26 April 2000; accepted 20 July 2000

Scanometric DNA Array Detection with Nanoparticle Probes

T. Andrew Taton,[1,2] Chad A. Mirkin,[1,2]* Robert L. Letsinger[1]*

A method for analyzing combinatorial DNA arrays using oligonucleotide-modified gold nanoparticle probes and a conventional flatbed scanner is described here. Labeling oligonucleotide targets with nanoparticle rather than fluorophore probes substantially alters the melting profiles of the targets from an array substrate. This difference permits the discrimination of an oligonucleotide sequence from targets with single nucleotide mismatches with a selectivity that is over three times that observed for fluorophore-labeled targets. In addition, when coupled with a signal amplification method based on nanoparticle-promoted reduction of silver(I), the sensitivity of this scanometric array detection system exceeds that of the analogous fluorophore system by two orders of magnitude.

Sequence-selective DNA detection has become increasingly important as scientists unravel the genetic basis of disease and use this new information to improve medical diagnosis and treatment. Commonly used heterogeneous DNA sequence detection systems, such as Southern blots and combinatorial DNA chips, rely on the specific hybridization of surface-bound, single-strand capture oligonucleotides to complementary targets. Both the specificity and sensitivity of these assays are dependent on the dissociation properties of capture strands hybridized to perfect and to mismatched complements. Recently, we developed a nanoparticle-based detection scheme that uses two gold particle probes with covalently bound oligonucleotides that are complementary to a target of interest (*1*–*3*). When encountering target strands, these particle probes are polymerized and form network structures composed of thousands of particles. In addition, the polymerization process is accompanied by a red-to-blue color change, providing a means of detection. These network structures exhibit exceptionally sharp melting profiles; the full width at half-maximum (FWHM) for the first derivatives of these melting transitions is as low as 2°C. Sharp melting transitions allow one to differentiate a perfectly complementary target strand from a strand with a single base mismatch, regardless of position on a 24-nucleotide sequence. The sharp melting in this nanoparticle network system as compared with normal DNA duplex melting as monitored by ultraviolet (UV)–visible absorption at 260 nm derives, in part, from: (i) a cooperative effect due to the multiple duplex interconnects between particles in the network structure, and (ii) the monitoring of a nanoparticle optical signature that is sensitive to interparticle distance and particle aggregate size rather than a DNA base signature. Here we report that the use of single-nanoparticle probes in recognizing DNA segments immobilized on a chip affords substantially sharper and higher temperature melting profiles than those obtained with analogous, conventional fluorophore-based systems. This observation, combined with (i) the development of a quantitative signal amplification method based on nanoparticle-promoted reduction of silver(I) and (ii) the use of a conventional flatbed scanner as a reader, have allowed us to develop a new "scanometric" chip-based detection system for DNA that has single mismatch selectivity and a sensitivity that, at present, is 100 times greater than that of conventional, analogous fluorescence-based assays as monitored by confocal fluorescence microscopy.

Gold nanoparticles modified with oligonucleotides (*3*) were used to indicate the presence of a particular DNA sequence hybridized on a transparent substrate in a three-component sandwich assay format (Scheme 1). In a typical experiment, target-active substrates were fabricated by attaching 3′-thiol–modified capture oligonucleotides to the surface of float glass microscope slides (Fisher Scientific, Pittsburgh, Pennsylvania) according to procedures from the

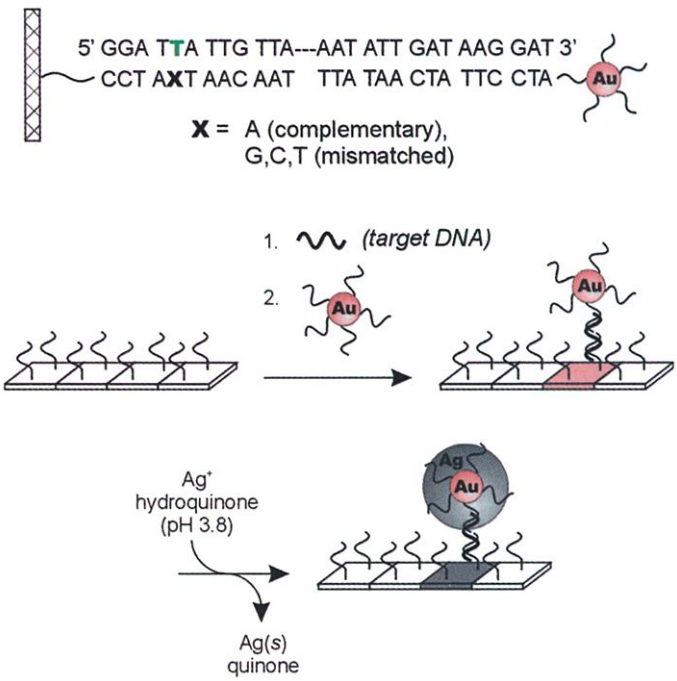

Scheme 1.

[1]Department of Chemistry, [2]Center for Nanofabrication and Molecular Self-Assembly, Northwestern University, Evanston, IL 60208, USA.

*To whom correspondence should be addressed. E-mail: camirkin@chem.northwestern.edu (C.A.M.); r-letsinger@chem.northwestern.edu (R.L.L.)

literature (*4*). In one set of experiments, the entire slide surface was modified with 12-base oligonucleotides of a given sequence; in another set, oligonucleotide arrays were generated by spotting various oligonucleotides with a commercial microarrayer. Nanoparticle probes and synthetic 27-base oligonucleotide targets (based on the anthrax lethal factor sequence) were then cohybridized to these substrates in buffer solution (Scheme 1). For tests at high target concentrations (≥1 nM), the high density of surface-hybridized nanoparticles made the surface appear light pink (Fig. 1, A and B). At lower target concentrations (≤100 pM), the attached nanoparticles could not be visualized with the naked eye (Fig. 1E), although they could be imaged by field-emission scanning electron microscopy (*5*). To facilitate visualization of nanoparticle labels hybridized to the array surface, we used a signal amplification method in which silver ions are reduced by hydroquinone to silver metal at the surfaces of the gold nanoparticles. This process increased the scanned intensity by a factor as large as 10^5. Although silver enhancement has been used to visualize protein-, antibody-, and DNA-conjugated gold nanoparticles in histochemical electron microscopy studies (*6*, *7*), it has not been used in quantitative DNA hybridization assays or combinatorial chip-based detection formats. We found that our scanometric detection method not only enabled very low surface coverages of nanoparticle probes to be visualized by a simple flatbed scanner or by the naked eye (Fig. 1, C and F) but also permitted the quantification of target hybridization on the basis of the imaged grayscale of the darkened area (Fig. 1H). In the absence of target or in the presence of noncomplementary target, no darkening of the surface was observed (Fig. 1G), demonstrating that neither nonspecific binding of nanoparticles to the surface nor nonspecific silver formation on bare glass occurs. Low nonspecific binding (in fact, undetectable with this technique) is an unusual feature of these heavily functionalized, oligonucleotide-nanoparticle conjugates (bearing approximately 220 oligonucleotides per 13-nm–diameter particle) (*8*), which enables ultrasensitive detection of DNA sequences.

We have found that oligonucleotide-functionalized nanoparticles exhibit unique hybridization properties that can lead to improved selectivity in assays on oligonucleotide arrays (or "gene chips") (*9*). The relative ratios of targets hybridized to different elements of an oligonucleotide array determine the effectiveness of the array in discriminating between different target sequences. In principle, the greater the difference in binding affinity at a given temperature between a complex containing a perfect target and one with a mismatched base, the higher this ratio and the better the discrimination. As a test of the relative selectivities of fluorophore and nanoparticle probes, we carried out experiments in which melting curves were obtained for surface-bound complexes comprising matched or mismatched capture oligonucleotides, a target oligonucleotide, and probes bearing either fluorophore or nanoparticle reporting groups (Scheme 1) (*10*). Although the fluorescein-labeled complexes dehybridized over a very broad temperature range (first derivative FWHM = 18°C), as expected for a complex containing a relatively small number of base pairs, the surface-bound complexes containing identical oligonucleotides but nanoparticle reporter groups melted over a very narrow temperature range (first derivative FWHM = 3°C). The sharp melting curves of the nanoparticle probe translate into high recognition selectivity, because a temperature can be selected so that a high proportion of labeled probe remains hybridized to perfectly matched capture strands while most of the probe is dehybridized from mismatched capture strands. (For the specific example in Fig. 2, 81% of the target was retained for the matched capture strand and only 19% for the mismatched capture strand at the stringency temperature shown.) The midpoint temperatures in the melting curves (T_m values) for the complexes with the nanoparticle probes also were significantly higher than the corresponding values for the fluorophore probes. This feature should increase the sensitivity achievable in the assay, because an increase in the melting temperature of the surface complex lowers the critical concentration below which the complex spontaneously melts at room temperature.

To evaluate the effectiveness of nanoparticles as scanometric indicators for oligonucleotide arrays, a synthetic target was hybridized to different capture strands immobilized onto glass chips and was then assayed separately with fluorophore and nanoparticle probes. The test arrays, the oligonucleotide target, and the Cy3 label strand (indodicarbocyanine 3; Cy3 is a trademark of Biological Detection Systems, now part of Amersham Pharmacia Biotech, Uppsala, Sweden) were made according to published protocols (*4*, *11*). Arrays contained four elements corresponding to each of the four possible nucleotides at position 5 of the target. The arrays were designed to evaluate discrimination between an A:T complement (X = A) and a G:T "wobble" pairing (X = G), a particularly difficult task for conventional fluorophore-based assays (*12*, *13*). The synthetic target and either fluorophore or nanoparticle probes were hybridized successively to arrays in hybridization buffer, and each step was followed with a stringency buffer wash (*14*). After the second wash, the arrays treated with nanoparticle probes were immersed in the silver am-

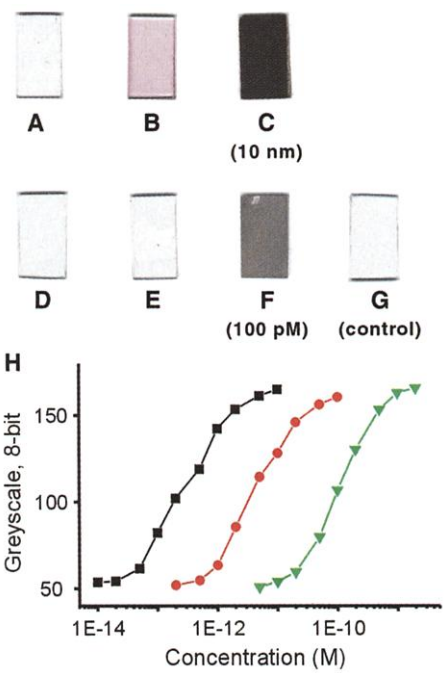

Fig. 1. Images of 7 mm by 13 mm, oligonucleotide-functionalized, float glass slides, obtained with a flatbed scanner. (**A**) Slide before hybridization of target and nanoparticle probe. (**B**) A slide identical to (A) after hybridization with oligonucleotide target (10 nM) and then nanoparticle probes (5 nM in particles). The pink color derives from the Au nanoparticle probes. (**C**) A slide identical to (B) after exposure to silver amplification solution for 5 min. (**D**) Slide before hybridization of target and nanoparticle probe. (**E**) A slide identical to (D) after hybridization with target (100 pM) and then nanoparticle probe (5 nM). The extinction of the submonolayer of nanoparticles is too low to be observed visually or with a flatbed scanner. (**F**) A slide identical to (E) after exposure to silver amplification solution for 5 min. Slide (F) is lighter than slide (C), indicating a lower concentration of target. (**G**) A control slide exposed to 5 nM nanoparticle probe and then exposed to silver amplification solution for 5 min. No darkening of the slide is observed. (**H**) Graph of 8-bit gray scale values as a function of target concentration. The gray scale values were taken from flatbed scanner images of oligonucleotide-functionalized glass surfaces that had been exposed to varying concentrations of oligonucleotide target, labeled with 5 nM oligonucleotide probe and immersed in silver amplification solution. For any given amplification time, the grayscale range is limited by surface saturation at high grayscale values and the sensitivity of the scanner at low values. Therefore, the dynamic range of this system can be adjusted by means of hybridization and amplification conditions (that is, lower target concentrations require longer amplification periods). Squares: 18-base capture-target overlap (*5*), 8× PBS hybridization buffer [1.2 M NaCl and 10 mM NaH_2PO_4/Na_2HPO_4 buffer (pH 7)], 15 min amplification time. Circles: 12-base capture-target overlap, 8× PBS hybridization buffer, 10 min amplification time. Triangles: 12-base capture-target overlap, 2× PBS hybridization buffer [0.3 M NaCl, 10 mM NaH_2PO_4/Na_2HPO_4 buffer (pH 7)], 5 min amplification time. The lowest target concentration that can be effectively distinguished from the background baseline is 50 fM.

plification solution for 5 min. Silver amplification darkened the array elements so that the 200-μm–diameter elements could be easily imaged with a flatbed scanner or even the naked eye.

Arrays challenged with the target and nanoparticle labels and amplified with the silver solution exhibited more selective hybridization to complementary array elements and higher signal intensity than did arrays challenged with target and fluorophore labels (Fig. 3). For both nanoparticle- and fluorophore-based arrays, a low-temperature wash did not dissociate the target from mismatched array elements and produced hybridization signal at all four elements. As the stringency temperature was increased, target dissociated from the different elements in the order of the predicted stability of the Watson-Crick base pairs (*15*): C:T and T:T mismatches first, followed by the G:T wobble pair, and finally by the A:T complement. It is clear that, as predicted by the dissociation curves (Fig. 2), these transitions occur much more sharply for the nanoparticle-labeled arrays than for the Cy3-labeled arrays (Fig. 3) (*16*). This sharpening has two important consequences with respect to the hybridization signal obtained at the optimum stringency temperature (shown by the dark boxes in Fig. 3). First, the relative signal intensity at the complementary (A) element versus the wobble (G) element is much greater for the nanoparticle-labeled array (Fig. 3, left) than for the fluorophore-labeled array (Fig. 3, right). This demonstrates the higher sequence selectivity of the array detection system based on nanoparticle probes. Although the fluorophore-based system shows 2.6:1 selectivity for the perfect complement at 35°C (the optimum stringency temperature), the nanoparticle-based system shows over 10:1 selectivity at 50°C (the optimum stringency temperature). Second, the absolute signal intensity at the complementary (A) element is greater for the nanoparticle array at the temperature of optimum stringency. As optimum stringency is approached with fluorophore probes, most of the hybridized target and label are dissociated from the array, leaving little signal to image. Note the decrease in signal as the temperature is increased from 15° to 35°C (Fig. 3, right). With nanoparticle probes, on the other hand, over 80% of the nanoparticle label is retained at the complementary element at stringency (Fig. 3, left, 50°C). Hybridization signal could be resolved at the X = A elements at target concentrations as low as 50 fM (*5*); this represents a 100-fold increase in sensitivity over that of Cy3-labeled arrays imaged by confocal fluorescence microscopy, for which target concentrations of 5 pM or greater were required. The higher melting temperatures observed for nanoparticle-target complexes immobilized on surfaces undoubtedly contributed to the sensitivity of the array. The greater stability of the probe/target/surface-oligonucleotide complex in the case of the nanoparticle system as compared with the fluorophore system presumably results in less target and probe lost during washing steps.

We expect that scanometric DNA array detection will be useful in applications such

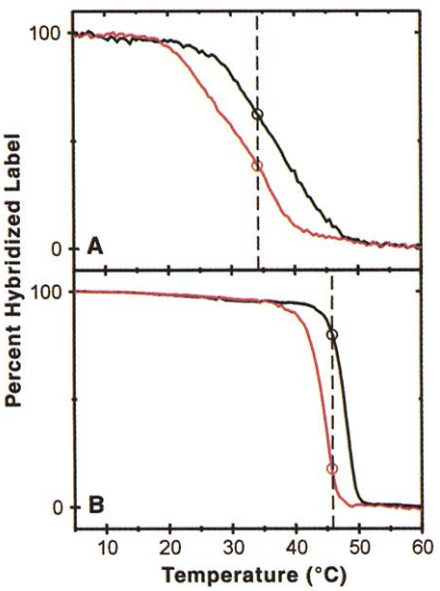

Fig. 2. (**A**) Dissociation of fluorescein-labeled target from the surfaces of oligonucleotide-functionalized glass beads, monitored by quantifying the fluorescence of the dissociated label at wavelength (λ) = 520 nm in the 2× PBS buffer solution (above the beads) as a function of temperature. The black curve describes the dissociation of target and probe from a perfectly complementary capture strand (Scheme 1, X = A; T_m = 37°C, first derivative FWHM = 18°C), and the red curve describes the analogous process for a capture strand with a single mismatch (Scheme 1, X = G; T_m = 32°C, first derivative FWHM = 19°C). The breadth of these curves is typical for dissociation of fluorophore-labeled targets from surface capture strands (*17*). The intercepts at the vertical dotted line in the graph can be used to estimate the expected relative fluorescence intensities at complementary and mismatched oligonucleotide array elements at a given temperature, and thus provide an estimate of the expected selectivity of sequence identification for fluorophore-based gene chips. In this case, halfway between the T_m's for the two curves (chosen arbitrarily), the expected ratio of fluorescence intensities is 62/38% = 1.6:1. (**B**) Dissociation of nanoparticle-labeled targets from the surfaces of oligonucleotide-functionalized glass beads, monitored by quantifying the absorbance of the dissociated label at λ = 520 nm (in the solution above the beads) as a function of temperature. The black curve describes the dissociation of target and nanoparticle probe from a perfectly complementary capture strand (Scheme 1, X = A; T_m = 48°C, first derivative FWHM = 3°C), and the red curve describes the analogous process for a capture strand with a single mismatch (Scheme 1, X = G; T_m = 45°C, first derivative FWHM = 3°C). The intercepts at the vertical dotted line allow one to estimate the expected ratio of nanoparticle label at complementary and mismatched array elements (at a temperature halfway between the T_m's for the two curves) and thus are an estimate of the expected selectivity of sequence identification for nanoparticle-based gene chips. At this temperature, this ratio is 81/19% = 4.3:1.

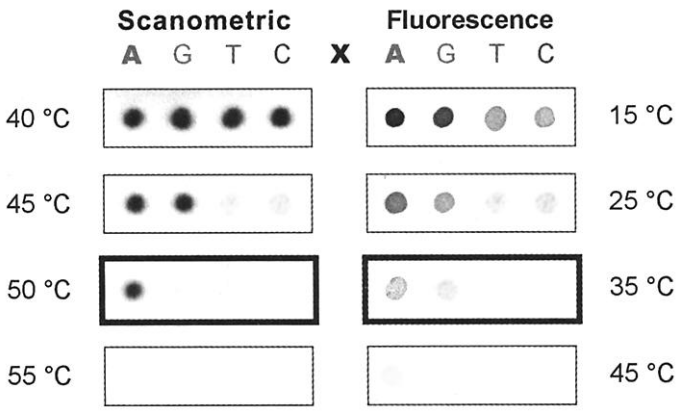

Fig. 3. (**Left**) Nanoparticle-labeled arrays developed at different stringency temperatures. Model oligonucleotide arrays (with the capture sequences shown in Scheme 1) were treated with oligonucleotide target and nanoparticle probes, followed by a 2-min buffer wash at the temperatures shown and subsequent silver amplification (*13*). Images were obtained with an Epson Expression 636 (600 dots per inch) flatbed scanner (Epson America, Long Beach, California). The darkened border indicates the array that showed optimum selectivity for the perfectly complementary target; at this temperature, the ratio of background-subtracted, 8-bit gray scale values for elements A:G:T:C, obtained from histogram averages in Adobe Photoshop (Adobe Systems, San Jose, California), is 96:9:7:6. (**Right**) Fluorophore-labeled arrays washed at different stringency temperatures. Model oligonucleotide arrays identical to those shown at left were treated with oligonucleotide target and Cy3-labeled oligonucleotide probes, followed by a 2-min buffer wash at the temperatures shown. Images were obtained with a ScanArray Confocal Microarray Scanner (GSI Lumonics, Billerica, Massachusetts). The darkened border indicates the array that showed the highest selectivity for the perfectly complementary target, as calculated by the QuantArray Analysis software package (GSI Lumonics); at this temperature, the intensity ratio (in percent, with the intensity of the X = A element at 15°C set to 100%) for elements A:G:T:C is 18:7:1:1.

as single-nucleotide polymorphism analysis, where single-mismatch resolution, sensitivity, cost, and ease of use are important factors. Moreover, the sensitivity of this system, which has yet to be totally optimized, points toward a potential method for detecting oligonucleotide targets without the need for target amplification schemes such as the polymerase chain reaction.

References and Notes

1. C. A. Mirkin, R. L. Letsinger, R. C. Mucic, J. J. Storhoff, *Nature* **382**, 607 (1996).
2. R. Elghanian, J. J. Storhoff, R. C. Mucic, R. L. Letsinger, C. A. Mirkin, *Science* **277**, 1078 (1997).
3. J. J. Storhoff, R. Elghanian, R. C. Mucic, C. A. Mirkin, R. L. Letsinger, *J. Am. Chem. Soc.* **120**, 1959 (1998).
4. L. A. Chrisey, G. U. Lee, C. E. O'Ferrall, *Nucleic Acids Res.* **24**, 3031 (1996).
5. Supplementary material is available at *Science* Online at www.sciencemag.org/feature/data/1051941.shl.
6. G. W. Hacker, in *Colloidal Gold: Principles, Methods, and Applications*, M. A. Hayat, Ed. (Academic Press, San Diego, CA, 1989), vol. 1, chap. 10.
7. I. Zehbe *et al.*, *Am. J. Pathol.* **150**, 1553 (1997).
8. R. C. Mucic, thesis, Northwestern University, Evanston, IL (1999).
9. For a review on oligonucleotide arrays, see S. P. A. Fodor, *Science* **277**, 393 (1997).
10. For the experiments reported in Fig. 2, dissociation measurements were made from the surface of glass beads 250 to 300 μm in diameter (Polysciences, Warrington, PA) rather than planar substrates to increase the UV-visible and fluorescence signal intensity.
11. 5′-Cy3–labeled oligonucleotide probes were synthesized on an Expedite automated synthesizer (Millipore, Bedford, MA) using Cy3 phosphoramidite (Glen Research, Sterling, VA) as the label source. Arrays of spots 175 μm in diameter separated by 375 μm were patterned with a GMS 417 Microarrayer (Genetic Microsystems, Woburn, MA).
12. R. K. Saiki and H. A. Erlich, in *Mutation Detection*, R. G. H. Cotton, E. Edkins, S. Forrest, Eds. (Oxford Univ. Press, Oxford, 1998), chap. 7.
13. S. Ikuta, K. Takagi, R. B. Wallace, K. Itakura, *Nucleic Acids Res.* **15**, 797 (1987).
14. First, 20 μl of a 1 nM solution of synthetic target in 2× phosphate-buffered saline (PBS) [0.3 M NaCl and 10 mM NaH_2PO_4/Na_2HPO_4 buffer (pH 7)] was hybridized to the array for 4 hours at 10°C in a CoverWell PC20 hybridization chamber (Grace Bio-Labs, Bend, OR) and was then washed at 10°C with clean PBS buffer. Next, 20 μl of a 100 pM solution of either oligonucleotide-functionalized gold nanoparticles or 5′-Cy3–labeled probe in 2× PBS was hybridized to the array for 4 hours at 10°C in a fresh hybridization chamber. The array was then washed at the stringency temperature (shown in Fig. 3) with clean 2× PBS buffer for 2 min. Arrays labeled with nanoparticle probes were washed twice at room temperature with 2× PBN [0.3 M $NaNO_3$ and 10 mM NaH_2PO_4/Na_2HPO_4 buffer (pH 7)], then submerged in Silver Enhancer Solution (Sigma) for 5 min at room temperature and washed with water.
15. H. T. Allawi and J. SantaLucia Jr., *Biochemistry* **36**, 10581 (1988).
16. The temperature ranges for the melting curves in Fig. 2 do not correspond exactly with the stringency temperatures associated with the oligonucleotide array experiments reported in Fig. 3. This is probably because the two sets of experiments are not identical with respect to the substrate.
17. J. E. Forman, I. D. Walton, D. Stern, R. P. Rava, M. O. Trulson, in *Molecular Modeling of Nucleic Acids*, N. B. Leontis and J. SantaLucia Jr., Eds. [American Chemical Society (ACS) Symposium Series 682, ACS, Washington, DC, 1998), pp. 206–228.

18. C.A.M. and R.L.L. acknowledge the Army Research Office (DAAG55-97-1-0133) and the National Institute of General Medical Sciences (GM 57356) for support of this work.

5 May 2000; accepted 19 July 2000

Printing Proteins as Microarrays for High-Throughput Function Determination

Gavin MacBeath[1]* and Stuart L. Schreiber[2]

Systematic efforts are currently under way to construct defined sets of cloned genes for high-throughput expression and purification of recombinant proteins. To facilitate subsequent studies of protein function, we have developed miniaturized assays that accommodate extremely low sample volumes and enable the rapid, simultaneous processing of thousands of proteins. A high-precision robot designed to manufacture complementary DNA microarrays was used to spot proteins onto chemically derivatized glass slides at extremely high spatial densities. The proteins attached covalently to the slide surface yet retained their ability to interact specifically with other proteins, or with small molecules, in solution. Three applications for protein microarrays were demonstrated: screening for protein-protein interactions, identifying the substrates of protein kinases, and identifying the protein targets of small molecules.

Historically, genome-wide screens for protein function have been carried out with random cDNA libraries. Most frequently, the libraries are prepared in phage vectors and the expressed proteins immobilized on a membrane by a plaque lift procedure. This method has been effective for a variety of applications (*1*–*4*), but it has several limitations. Most clones in the library do not encode proteins in the correct reading frame, and most proteins are not full-length. Bacterial expression of eukaryotic genes frequently fails to yield correctly folded proteins, and products derived from abundant transcripts are overrepresented. Moreover, because plaque lifts are not amenable to miniaturization on the micrometer scale, it is hard to imagine screening all the proteins of an organism hundreds or thousands of times by this approach.

With the advent of high-throughput molecular biology, it is now possible to prepare large, normalized collections of cloned genes. UniGene sets in the form of polymerase chain reaction products have been used extensively over the past decade to construct DNA microarrays for the study of transcriptional regulation (*5*). Recently, spatially segregated clones in expression vectors were used to study protein function in vivo using the yeast two-hybrid system (*6*) and in vitro using biochemical assays (*7*). We have built on these efforts by developing microarray-based methods to study protein function.

To accomplish these goals, it is necessary to immobilize proteins on a solid support in a way that preserves their folded conformations. One group has described methods of arraying functionally active proteins, using microfabricated polyacrylamide gel pads to capture their samples and microelectrophoresis to accelerate diffusion (*8*). In contrast, we have immobilized proteins by covalently attaching them to the smooth, flat surface of glass microscope slides. One of our primary objectives in pursuing this approach was to make the technology easily accessible and compatible with standard instrumentation. We use a variety of chemically derivatized slides that can be printed and imaged by commercially available arrayers and scanners. For most applications, we use slides that have been treated with an aldehyde-containing silane reagent (*9*). The aldehydes react readily with primary amines on the proteins to form a Schiff's base linkage. Because typical proteins display many lysines on their surfaces as well as the generally more reactive α-amine at their NH_2-termini, they can attach to the slide in a variety of orientations, permitting different sides of the protein to interact with other proteins or small molecules in solution.

To fabricate protein microarrays, we use a high-precision contact-printing robot (*10*) to deliver nanoliter volumes of protein samples to the slides, yielding spots about 150 to 200 μm in diameter (1600 spots per square centimeter). The proteins are printed in phosphate-buffered saline with 40% glycerol included to prevent evaporation of the nanodroplets. It is important that the proteins remain hydrated throughout this and subsequent steps to prevent denaturation. After a 3-hour incubation, the slides are immersed in a buffer containing bovine serum albumin (BSA). This step not only quenches the unreacted aldehydes on the slide, but also forms a molecular layer of BSA that reduces nonspecific binding of other proteins in subsequent steps.

Although appropriate for most applications, aldehyde slides cannot be used when peptides

[1]Center for Genomics Research, Harvard University, 16 Divinity Avenue, Cambridge, MA 02138, USA. [2]Howard Hughes Medical Institute (HHMI), Department of Chemistry and Chemical Biology, Harvard University, 12 Oxford Street, Cambridge, MA 02138, USA.

*To whom correspondence should be addressed. E-mail: gavin_macbeath@harvard.edu